Viscoelastic Properties of Isomeric Alkylglucoside Surfactants Studied by Surface Light Scattering

Orlando J. Rojas,*,† Ronald D. Neuman,‡ and Per M. Claesson§

Forest Biomaterials Laboratory, College of Natural Resources, North Carolina State University, Box 8005, Raleigh, North Carolina 27695, Department of Chemical Engineering, Auburn University, Auburn, Alabama 36849, and Department of Chemistry, Surface Chemistry, Royal Institute of Technology KTH, SE-100 44 and Institute for Surface Chemistry YKI, Box 5607, SE-114 86, Stockholm, Sweden

Received: July 26, 2005; In Final Form: September 19, 2005

Surface light scattering (SLS) by capillary waves was used to investigate the adsorption behavior of nonionic sugar surfactants at the air/liquid interface. SLS by the subphase (water) followed predictions from hydrodynamic theory. The viscoelastic properties (surface elasticity and surface viscosity) of monolayers formed by octyl β-glucoside, octyl α-glucoside, and 2-ethylhexyl α-glucoside surfactants were quantified at submicellar concentrations. It is further concluded that a diffusional relaxation model describes the observed trends in high-frequency, nonintrusive laser light scattering experiments. The interfacial diffusion coefficients that resulted from fitting this diffusional relaxation model to surface elasticity values obtained with SLS reflect the molecular dynamics of the subphase near the interface. However, differences from the theoretical predictions indicate the existence of effects not accounted for such as thermal convection, molecular rearrangements, and other relaxation mechanisms within the monolayer. Our results demonstrate important differences in molecular packing at the air−water interface for the studied isomeric surfactants.

Introduction

Properties such as interfacial tension and surface viscoelasticity are essential to the understanding of the behaviors of self-assembled monolayers and thin films as well as their contribution in foaming, detergency, and emulsification. These properties not only reflect the conformation, interaction, and packing of the adsorbed species but are highly relevant to both equilibrium and dynamic surface phenomena.

One of the various methods to measure the surface tension and viscoelasticity of surfactant and polymer solutions is through the analysis of surface capillary waves. High-frequency capillary waves are known to be responsible for spontaneous perturbations of interfaces leading to film rupture and other important effects.[1] The study of capillary waves by nondisturbing techniques such as Surface Light Scattering (SLS) was first introduced in 1967 by Katyl and Ingard[2] and since then has been used in several studies, mainly dealing with insoluble surfactant monolayers and polymer films.

SLS covers a rather different time scale as compared to other (e.g., mechanical, acoustical, or electrical) methods. Furthermore, SLS can access surface properties that at present are not otherwise measurable with other techniques.[3,4] Nonintrusive SLS measurements are averaged over areas (probed by the laser beam) that are much smaller than the entire surface. This is in contrast to other techniques that involve either slow macroscopic perturbations or more rapid motion of molecular probes influenced by the immediate molecular environment.[5] SLS experiments allow the quantification of the fluctuations in intensity of the light scattered by thermally excited capillary waves. These capillary waves are created by the local thermal fluctuation at the air/liquid interface and typically have an amplitude and wavelength of ca. 2 Å and 100 μm, respectively.[3,4,6,7] In SLS experiments the time evolution of capillary waves of selected wavelength is investigated by measuring their complex frequency as a function of the wavenumber (k). This is in contrast to electrocapillary wave diffraction or other techniques where surface waves are generated at fixed frequencies and the complex wavenumber k is measured.[8]

The viscoelastic properties of monolayers composed of insoluble surface-active molecules have attracted significant attention in recent years. However, after the first reported light-scattering measurements in 1987 by Hård et al.[9] very few studies on SLS of soluble monolayers were made available.[10−12] Interestingly, octyl glucoside surfactants tend to produce viscous films at interfaces, probably due to the strong hydrogen bonding interaction between the glucoside groups at the interface. However, despite the wide-ranging research work carried out on the bulk and interfacial properties of alkylglucoside (sugar) surfactants,[13−16] to our knowledge their surface rheological properties by high-frequency experiments have not been identified so far. This is surprising since these surfactants (or sugar surfactants) are being used in numerous commercial applications where the (surface) rheological behavior is of utmost importance.

A detailed description of surface rheology and the theory of capillary waves and measuring principles are beyond the scope of this paper, and the reader is referred to review articles on the subject.[1,3,4,17−20] Nevertheless, the following sections are presented for a better understanding of the diffusional viscoelasticity model used to interpret our results from SLS experiments.

Surface Properties and Diffusional Viscoelasticity Models. The estimation of viscoelastic properties of surfactant monolayers involves different models and the use of equilibrium

* Address correspondence to this author. Phone: +1-919-513 7494. Fax: +1-919-515 6302. E-mail: ojrojas@ncsu.edu.
† North Carolina State University.
‡ Auburn University.
§ Royal Institute of Technology KTH, SE-100 44 and Institute for Surface Chemistry YKI.

10.1021/jp054132w CCC: $30.25
Published on Web 10/27/2005

values that are usually calculated from a priori knowledge of the adsorption behavior of the surfactant as accounted by the adsorption isotherm or equation of state. Here it was assumed that the Frumkin equation of state described the surface tension data of the studied surfactants. This equation was proposed by Frumkin in 1925 for fatty acids[21] and later used by Lucassen and Hansen.[22] More recently it was used in the context of laser light scattering interpretation by other researchers.[10,23−26] In the Frumkin equation a nonideality parameter arising from the interactions between the adsorbed species in the monolayer is included, H^S. This parameter vanishes in the limit of Langmuir−Szyszkowski[27] adsorption (perfect surface mixing).[22,23,28−30] By using the Gibbs adsorption equation the equilibrium adsorption isotherm (in the Frumkin framework) can be derived and used in the computation of ripple characteristics of adsorbed monolayers as a function of the surfactant concentration.

Viscoelasticity. Rayleigh[31] and Gibbs[32] provided the basis for quantitative interpretation of the effects caused by gradients in surface tension by defining a surface elasticity ϵ (also called "Gibbs elasticity", "areal elasticity", "compressional modulus", or "film elasticity") as the increase in surface tension γ per unit of relative increase in surface area A. Gibbs defined this parameter for the surface of a soap-stabilized liquid film, but it turns out to be the appropriate parameter to express surface tension gradients in any liquid interface. The modulus ϵ is a measure of the resistance against the creation of surface tension gradients, and of the rate at which such gradients disappear once the system is again left to itself.[23]

The application of hydrodynamic theories to capillary waves is too elaborate and rather involved to be presented here and the reader is referred to classical texts.[33−35] Four formal rheological coefficients are needed for the description of the surface tensor, the surface dilatational elasticity, ϵ_d, and the surface dilatational viscosity, η_d, which account for the surface resistance against changes in area. On the other hand the surface shear elasticity, ϵ_s, and the surface shear viscosity, η_s, describe the resistance against changes in shape of the surface element.

It is usually convenient to make the assumption that the shear components are negligible compared to the dilatational components.[20,36] If the shear components are neglected the surface stress tensor is now isotropic and therefore the varying surface stress can be described by a gradient in surface tension, which can be expressed in a surface dilatational modulus ϵ defined as

$$\epsilon = \epsilon_d + i\omega\eta_d = \frac{d\gamma}{d \ln A} \tag{1}$$

ϵ in periodic deformations is therefore a complex number (both in the case of elastic and viscous contributions). Its real part (storage modulus) is equal to the surface dilatational elasticity ϵ_d, and its imaginary part (loss modulus) is proportional to the surface dilatational viscosity η_d.[23]

For an arbitrary deformation, the surface dilatational coefficients, ϵ_d and η_d, will vary with the extent of compression or expansion of the surface element. However, in a given experiment with small fluctuations around the equilibrium state such as those obtained by propagating a wave over the surface with small amplitude:wavelength ratio, the surface dilatational coefficients are single valued. Also, the values of ϵ, ϵ_d, and η_d depend on the frequency of the wave motion.

In surfactant solutions diffusional interchange between the undulating surface and the bulk solution causes the total amount adsorbed in a surface element to depend on the time scale of the deformation process, in other words, on the frequency of the wave.[17] As a result, the surface dilatational modulus ϵ will depend on the wave frequency while the surface dilatational viscosity η_d is not negligible.

In viscoelasticity due to diffusional interchange it is assumed that local thermodynamic equilibrium is maintained at the surface. In other words, during surface expansion and contraction the surface tension instantaneously adjusts itself to the locally varying adsorption, which in turn is in equilibrium with the surfactant concentration immediately below the surface. If the establishment of this local equilibrium at the surface is not instantaneous, this means that another rate-dependent process, such as molecular rearrangements within the monolayer to a given adsorption, gives rise to surface dilatational viscosity.[17]

Relaxation by Diffusional Interchange. During contractions and expansions of the surface the relaxation processes that take place can be described by a diffusional interchange model. This model was discussed by Lucassen et al.[28,37] and includes similar derivations as those reported previously.[33,38−40] A review in light of this study can be found in Lucassen-Reynders and Lucassen.[17] The main idea is that the surface tension gradients, which occur during expansions or contractions, are more or less "short-circuited" due to the exchange of surface-active components between the surface and the bulk, thereby the absolute value of the surface dilatational modulus is lowered. The effect of the diffusion is then to transport matter between the (sub) surface and deeper layers. To find the surface dilatational modulus ϵ, it is first expressed as a function of the surfactant adsorption Γ, which is considered under local equilibrium with γ, and therefore the unknowns can be calculated by using Fick's diffusion law.

The calculation is simplified if the convective terms are neglected (which is reasonable since convection is very small for the low amplitude waves dealt with). By using appropriate boundary conditions the general solution for the diffusion equation is obtained and the complex surface dilatational modulus is obtained. This complex modulus can be split up into a real and an imaginary part. The real part represents the surface dilatational elasticity ϵ_d (eq 2):

$$\epsilon_d = \frac{-d\gamma}{d \ln \Gamma} \frac{1 + \tau}{1 + 2\tau + 2\tau^2} \tag{2}$$

where the effect of diffusion is accounted for by the parameter τ (eq 3):

$$\tau = \frac{dC}{d\Gamma}\sqrt{\frac{D}{2\omega}} = \sqrt{\frac{\omega_c}{\omega}} \tag{3}$$

Here C is the surfactant concentration and ω_c is a characteristic frequency for the diffusion introduced by Lucassen-Reynders[23] and later adapted in refs 24−26. ω_c can be written as (eq 4),

$$\omega_c = \frac{D}{2}\left(\frac{dC}{d\Gamma}\right)^2 \tag{4}$$

The imaginary part of ϵ represents the product of the frequency ω and the surface dilatational viscosity η_d (eq 5):

$$\eta_d = \frac{-d\gamma}{d \ln \Gamma} \frac{\tau}{\omega(1 + 2\tau + 2\tau^2)} \tag{5}$$

The first term that appears in both coefficients of eqs 2 and 5 is ϵ_0 or, equivalently, ϵ_∞. The diffusion parameter τ vanishes for insoluble monolayers (where $C = 0$). For soluble monolayers, the effect of diffusion (nonzero values of τ) on the elasticity, ϵ_d, is a progressive drop below the ϵ_0 values, even to

the point of null elasticity at high τ. The effect of increasing diffusional interchange on the viscosity, η_d, is an increase in η_d at low values of τ and a subsequent decrease, down to zero, at very high τ.

In the limit of very low wave frequency or very high concentrations any surface tension gradient is completely leveled out by diffusion to and from the surface during the time of measurement, i.e., during a period of ω^{-1} s. In this case the surface behaves as if it were pure, though with a much lower surface tension than that of a really pure surface. For negligible diffusion, or very high wave frequency ($\epsilon \rightarrow \infty$), the viscosity vanishes and the surface behaves purely elastically, with a modulus exclusively depending on equilibrium surface properties, i.e., ϵ_d ($=\epsilon_0$) and $\eta_d = 0$. This is the reason in some literature the limiting elasticity is identified in the context of capillary wave techniques with the symbol ϵ_∞ rather than ϵ_0.

In the general case the use of an equation of state provides the equilibrium values $-d\gamma/d \ln \Gamma$. For the Frumkin equation the characteristic frequency ω_c is calculated from the $C-\Gamma$ relationship as has been done by Lucassen-Reynders and Lucassen,[17] and more recently by other authors[10,24−26] (eq 6):

$$\omega_c = \frac{D}{2}\left[\frac{C}{\Gamma^\infty}\left[\frac{1}{\frac{\Gamma}{\Gamma^\infty}\left(1-\frac{\Gamma}{\Gamma^\infty}\right)}\right] - \frac{2H^S}{RT}\right] \quad (6)$$

where Γ^∞ is the saturation surface concentration and H^S is a nonideality parameter arising from the interactions between the adsorbed species in the monolayer, which vanishes in the limit of Langmuir-Szyszkowski adsorption (perfect surface mixing).[22,23]

In this study we compare the viscoelastic behavior of soluble monolayers from three nonionic, isomeric alkylglucoside surfactants using the framework of the diffusional viscoelastic model presented before. The underlying question is to what extent changes in the molecular structure of the surfactant affect their monolayer behavior, especially their viscoelastic properties. We report first experiments with pure water for validation of the SLS setup and then discuss the results for aqueous solutions of the soluble sugar surfactants at submicellar concentrations. Finally, we rationalize our results in light of the diffusional-relaxation behaviors for soluble monolayers.

Experimental Section

Sugar Surfactant Solutions. Straight-chain octyl glucoside surfactants, octyl β-glucoside (referred thereafter as "beta" or C8β) and octyl α-glucoside (referred thereafter as "alpha" or C8α), were obtained from Sigma (purity >98%) and used as supplied. Anomerically pure 2-ethylhexyl α-glucoside (purity >98%), which is a branched octyl glucoside surfactant (referred thereafter to as "branched" or 2EHα), was synthesized by Akzo Nobel Surface Chemistry AB (Stenungsund, Sweden) (see Figure 1).

Potassium bromide (pro-analysis grade) from Merck was roasted at 500 °C for 24 h before use. Special consideration was given to the purity of the water employed to check the SLS setup, and also in the preparation of the surfactant solutions. Tap water was first passed through a 50-μm dirt/rust water filter (AMF Cuno), a 20-μm colloidal filter, a water softener, and an activated carbon filter. After this pretreatment the water was passed through a reverse osmosis system and circulated through two deionization columns, an organic adsorption column (Super-Q), and a Millipore 0.2-μm filter before a two-stage distillation system (distillation with 0.15 M NaOH and 0.006 M potassium permanganate followed by a conventional stage). Only water freshly obtained after these purification steps was used in our experiments.

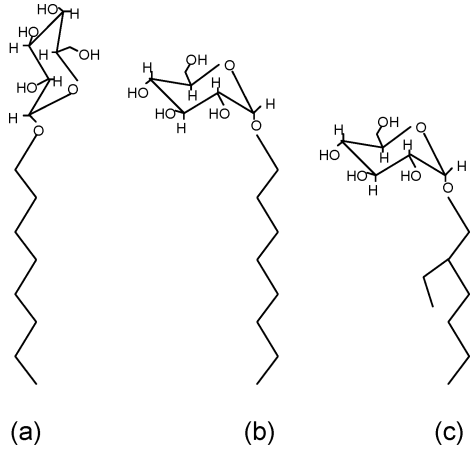

Figure 1. Octyl β-glucoside (C8β) (a), octyl α-glucoside (C8α) (b), and 2-ethylhexyl α-glucoside (2EHα)(c).

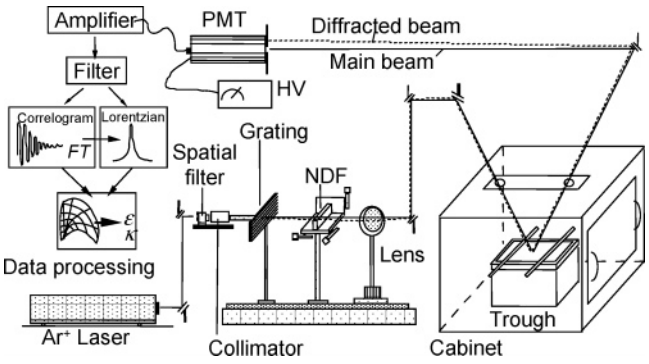

Figure 2. Schematic illustration of the SLS setup. PMT is a photomultiplier tube, HV is a high voltage generator and ϵ and κ are the viscoelastic coefficients obtained from the correlograms or Lorentzian functions after Fourier transformation (FT) (see later sections).

Surface Light Scattering Technique. The SLS setup employed in this study is similar to that used by Hård[41] (see Figure 2). The respective surfactant solution was placed inside a closed 316-stainless steel double-walled thermostated cabinet ($50 \times 50 \times 36$ cm^3) sitting on an optical table. The temperature was monitored by temperature probes located inside the chamber and maintained by an external thermostated circulation bath (to ±0.1 °C) and the humidity was set close to saturation (ca. 90% RH) by placing filter papers damped with water.

The experimental autocorrelation function, $G(\tau)$, of the surface waves followed an exponentially damped cosine function.[42] We digitally Fourier transformed the correlograms and then fitted them to a four-parameter Lorentzian function.[41,43] From these fittings we obtained the parameters of the power spectrum $P(w)$ (eq 7):

$$P(\omega) = \frac{A}{(\omega-\omega_0)^2 + \alpha^2} + B \quad (7)$$

where A, B, ω_0, and α are the amplitude, baseline, central frequency, and half-width at half-height frequency of $P(\omega)$, respectively. Figure 3 shows a typical spectrum from the correlator (after Fourier transforming the correlogram) together with a Lorentzian fit.

Theoretical Power Spectrum. The measured power spectrum was compared to the theoretical power spectrum ($P(\omega)$)

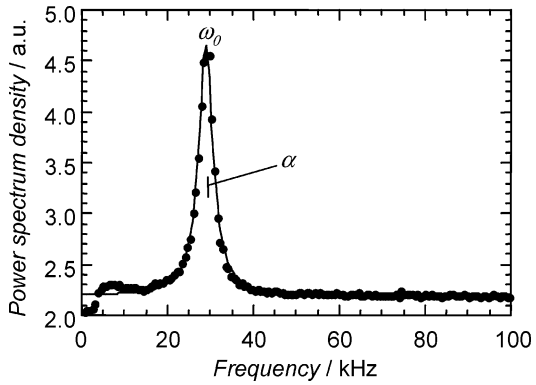

Figure 3. Power spectrum after Fourier transforming a SLS correlogram. A Lorentzian fit is shown with central frequency ω_o and half-width at half-height, α.

equation of Kramer (see ref 44) for capillary waves in the presence of air (eq 8). This theoretical power spectrum is described in terms of temperature, T, the wavelength of the measured surface waves, λ or wavenumber ($k = 2\pi/\lambda$), the bulk density ρ_j, and shear viscosity, η_j. It also takes into account the surface tension γ, the transverse viscosity μ, the sum of interfacial shear elasticity and interfacial dilatational elasticity ϵ, and the sum of interfacial shear viscosity and interfacial dilatational viscosity κ. Note that this equation is equivalent to the Lucassen-Reynders−Lucassen dispersion equation[17] also used by other investigators.[45]

$$P(\omega) = \frac{k_B T}{\pi\omega} \cdot \mathrm{Im}\left(\frac{1}{i\omega} \cdot \frac{X_1}{X_1 X_3 - X_2^2}\right) \tag{8}$$

where

$$X_1 = \eta_1(k + m_1) + \eta_2(k + m_2) - \frac{\epsilon^* k^2}{i\omega} \tag{9}$$

$$X_2 = \eta_1(k - m_1) - \eta_2(k - m_2) \tag{10}$$

$$X_3 = \eta_1\frac{m_1}{k}(k + m_1) + \eta_2\frac{m_2}{k}(k + m_2) - \frac{\gamma^* k^2}{i\omega} \tag{11}$$

and

$$\omega = \omega_0 - i\alpha \tag{12}$$

$$\epsilon^* = \epsilon - i\omega\kappa \tag{13}$$

$$\gamma^* = \gamma - i\omega\mu \tag{14}$$

$$m_j = \left[k^2 - \frac{i\omega\rho_j}{\eta_j}\right]^{1/2} \tag{15}$$

The experimental data, i.e., the central frequency and the damping coefficient (after correction for instrumental broadening), together with the bulk properties of the fluids were used to calculate the viscoelasticity coefficients from the power spectrum equation. Hence, the sum of shear and dilatational (elasticity and viscosity) was obtained. However, note that the shear components are orders of magnitude smaller than the dilatational ones and therefore they can be neglected.[20,36,45−47]

We used polar diagrams for direct interpretation of the rheological parameters ϵ and κ.[9] These plots (see, for example, Figure 8) are constructed from the dispersion equation for a given temperature, wavenumber, and surface tension (or surface pressure) by using as parameters the normalized complex frequency (ω_0/ω_w, α/α_w), where ω_0 is the experimental central frequency and α is the damping coefficient. Here the subscript "w" is used to denote the experimental values for a film-free surface ($\epsilon = 0$, $\kappa = 0$), i.e., water in our case.

The wavenumber k of the capillary waves must be accurately known to calculate the rheological coefficients of the monolayer at the interface. This evaluation was accomplished through determination of the scattering angle, which is defined by the transmission grating.

The determination of k is rather difficult because the scattering angle is very small (<1° for the employed diffraction orders). However, we estimated the wavenumber with accuracy better than 0.2% by the use of a reference grating within the Fraunhofer approximation.[41] For the different diffraction orders (3rd, 4th, and 5th) the calculated k values were 78 507.9, 105 356, and 131 492.8 m^{-1}, respectively. The wavenumber inaccuracy was estimated to be ±0.2% based on related uncertainties and on the spread of data in independent spot measurements. The error in the capillary wavenumber determination due to finite size of the diffraction spot was estimated to be less than 0.01% and therefore it is safe to neglect the spread of wavenumbers.

Results and Discussion

Surface Tension and Surface Excess. Surface tensions for aqueous solutions of C8β, C8α, and 2EHα with 0.1 mM KBr background concentration at 22 ± 0.1 °C were measured below the critical micelle concentration by using the technique of Wilhelmy (Sigma 70, KSV Instruments Ltd). The Wilhelmy plate consisted of a sandblasted (10 μm particle size) microscope cover glass of about 3.6 cm perimeter. Equilibrium times of at least 1 h were allowed and zero-buoyancy corrections were made.

Calculations of the surface elasticity and viscosity using the power spectrum equation show that the computed values are very sensitive to changes in the experimental parameters (central frequency, damping, and surface tension). Small differences in surface tension (which is the least accurate of the three) produce a shift in the location of the "isovisc" and "isoelast" lines of the polar diagram (see later sections). It is thus desirable to measure (under the same conditions as used in the SLS experiments) the surface tension as accurately as possible.

To overcome this difficulty Jiang et al.[48] employed a method proposed by Lucassen and Hansen[28] where the surface viscosity is assumed to be null and the surface elasticity and surface tension are obtained from the power spectrum equation (i.e., the surface tension is no longer an independent variable). This approach cannot be applied in this study because it depends on the assumptions that (a) equilibrium is established immediately in the interfacial region between surface tension and adsorption and (b) diffusional interchange between the bulk and the surface is negligible, i.e., the relaxation frequency is much smaller than the experimental frequency (or the inverse if one refers to the characteristic times), which in our experiments is only true at very low surfactant concentrations.

Therefore, to calculate the surface elasticity and surface viscosity from our SLS measurements the experimental surface tension values were used as inputs in the respective equations. Similarly, the experimental values were used in the prediction of the viscoelastic properties of the surfactants at submicellar concentrations based on the diffusional-relaxation model.

The adsorption isotherms for the three sugar surfactants were fitted to a fourth-order-polynomial equation with good agreement; however, it was noticed that the use of the Frumkin

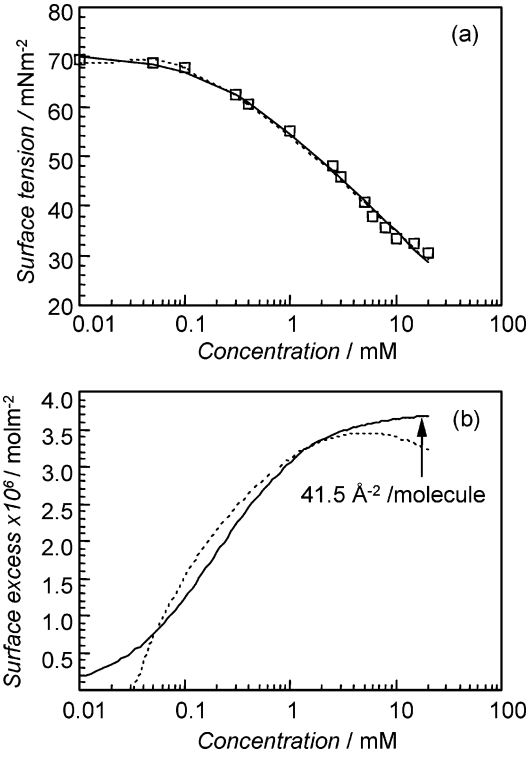

Figure 4. Surface tension (a) and surface excess (b) for octyl β-glucoside surfactant at 22 C and 0.1 mM KBr background concentration. A polynomial (broken line) and a Frumkin equation fit (continuous line) are also included. An area per molecule of 41.5 Å^2 is obtained.

equation of state provided a better fit. Small differences in the fit were noticed to produce remarkable differences in the surface excess values as calculated from the Gibbs equation. This fact and its effect on rheological calculations have been discussed elsewhere.[22,24,49]

Figure 4a includes the surface tension curve along with the calculated values from polynomial and Frumkin fits for C8β. Similar curves were obtained for the alpha and branched versions (not show). The surface excess curves according to the Gibbs equation for the polynomial and Frumkin fits are included in Figure 4b for C8β. We observed that the surface excess is slightly higher for the C8α surfactant, with C8β giving the smallest molecular packing at the surface. The Frumkin equation was chosen to describe the adsorption of the surfactants at the interface since the norm of the deviations was smaller.

Matsumara et al.[50] reported for decyl α-glucoside and decyl-β glucoside an area per molecule at saturation of 49 Å^2 (for both types of surfactants). In our case, the area per molecule was found to be 41.5 (octyl α-glucoside surfactant) and 43.5 Å^2 (octyl-β glucoside). Note that other techniques such as neutron reflection[49,51] may produce slightly different values to those obtained by surface tension.[49]

Technique Validation. Calibration of the SLS setup can be performed by using known values for the surface tension of water (or other known fluid).[8,45] However, our measurements were absolute, i.e., we did not use calibration fluids. Measurements of SLS (central frequencies and damping coefficients) by water were compared to those calculated from the power spectrum equation.

Signals from the 3rd, 4th, and 5th diffraction orders were recorded for high-purity water. In each case a new surface was produced by sweeping the water surface with Teflon barriers connected to movable bars that were manipulated from outside the chamber holding the sample (thus avoiding the risks of exposing the surfaces to external air).

TABLE 1: Comparison between Experimental and Theoretical (from the power spectrum equation) Complex Frequency for Water at 25.22 °C

Central Frequency			
diffraction order	exptl ω_0, Hz	theoretical ω_{0T}, Hz	% deviation
3	29 439.56	29 406.23	0.1
4	45 360.61	45 597.41	−0.5
5	63 433.82	63 427.30	0.01
Damping Coefficient			
diffraction order	exptl α, Hz	theoretical α_T, Hz	% deviation
3	1 616.44	1 558.83	3.7
4	2 792.77	2 775.34	0.6
5	4 355.02	4 284.01	1.7

The experimental values for the central frequency, ω_0, and the damping coefficient, α, are presented in Table 1 for water at 25.22 °C (after instrumental broadening correction). The theoretical values for the central frequency and damping coefficient, ω_{0T} and α_T, respectively, were computed from the power spectrum equation by using zero surface elasticity and zero surface viscosity. In the theoretical computation standard figures for water bulk properties (surface tension, viscosity and density) were used.

The experimental deviation for measurements of the central frequency is about 0.3%, and that for the damping coefficient is about 4%, therefore the differences seen in Table 1 are within the experimental error and thus there is excellent agreement with the theoretical predictions from the power spectrum equation. No excess damping was observed for water and the correlation between the experimental and the theoretical predictions indicates the proper setting and alignment of the SLS apparatus.

SLS Surface Viscoelasticity of Glucoside Surfactants. The central frequency and the damping coefficient are the two parameters obtained from the power spectra and are considered the primary data from which the rheological parameters are extracted. Figure 5a shows the experimental central frequency of the thermally generated capillary waves of the C8β surfactant as obtained by SLS using the 3rd, 4th, and 5th diffraction orders. Similar trends were obtained for the alpha and branched surfactants (not shown). No appreciable differences in the measured central frequencies for the three sugar surfactants were observed. The central frequency curves are similar to those obtained for surface tension, e.g., break in the curve for the beta surfactant is observed at a concentration corresponding to the cmc (as measured using tensiometry).

Figure 5b shows the damping coefficient, after correction for instrumental broadening of the measured half-width at half-height of the respective power spectra for C8β surfactant (for the 3rd, 4th, and 5th diffraction orders). A peak in the damping coefficient is seen well below the cmc region. This peak has been reported to arise from the coupling or resonance of longitudinal (dilatational) and transverse (capillary) modes.[8,45] Similar patterns were observed for the other two surfactants (data not shown).

The surface elasticity and surface viscosity were derived by using the diffusional-interchange model as explained in previous sections. The procedure first involved the calculation of the limiting (static or Gibbs) elasticity (ϵ_∞ or ϵ_0). The calculation of this equilibrium quantity was performed by fitting the surface excess data to the Frumkin equation of state.

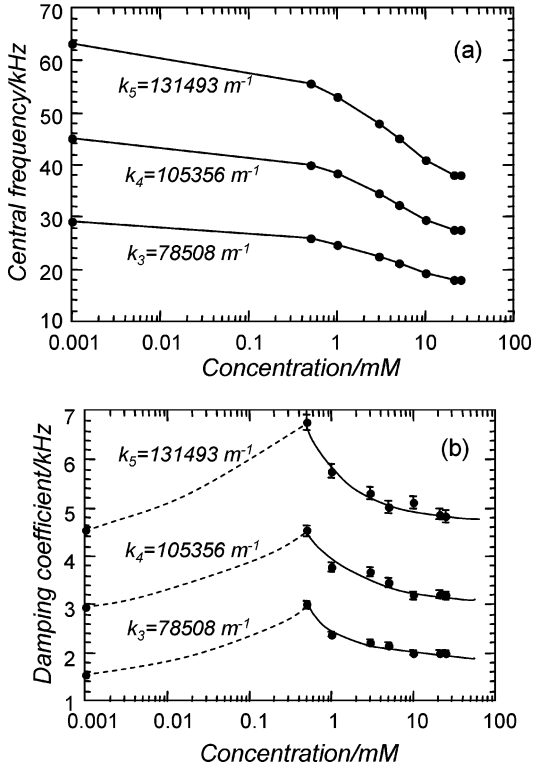

Figure 5. Central frequency (a) and damping coefficient (b) for capillary waves of octyl β-glucoside surfactant solutions (0.1 mM KBr background electrolyte) at three different wavenumbers. The experimental error in the central frequency is equivalent to a segment smaller than the respective symbol. In the case of the damping coefficients the experimental errors are equivalent to the vertical bars for each data point.

The fitting parameters in this equation are subsequently used in the expression for ϵ_0 derived after applying the Gibbs equation. ϵ_0 provides a limiting value for comparison purposes and represents the elasticity the film would have if there were no internal relaxation, e.g., in the case of an insoluble monolayer or for experiments at infinite frequencies (where the relaxation time, t_{rel}, is much higher than the characteristic time of the experiment, t_{exp}).

The surface-to-bulk exchange described by a Fickean diffusional process is incorporated in the diffusional model, and as explained before, the predictions of the surface properties are easily accessible through ϵ_d and η_d (or κ), the real and imaginary components of the complex elasticity modulus ($\epsilon = \epsilon_d + i\omega\kappa$) (the surface elasticity and surface viscosity, respectively). In these expressions the value of τ is computed from eq 3 with the experimental frequency, ω, as the value for the central frequency as measured by SLS, and the characteristic relaxation frequency, ω_c, from eq 6.

Figure 6 shows the predicted values for ϵ_d and $\omega\kappa$ at frequencies corresponding to capillary waves with a wavenumber of 78 508 m^{-1} (3rd diffraction order) for octyl β-glucoside surfactant. The limiting elasticity, ϵ_o, as obtained from equilibrium surface tension measurements, is also included. Similar behavior is noted for octyl α-glucoside and 2-ethylhexyl α-glucoside surfactants (not shown).

The diffusion coefficients used in the calculations were estimated from reported values found in the literature for the monomeric surfactants. van Buuren and Berendsen[52] used in their molecular dynamics simulation of decyl-glucoside surfactants values of $(4 \pm 1) \times 10^{-10}$ and $(3 \pm 1) \times 10^{-10}$ m^2/s for the alpha and beta surfactats isomers, respectively. Nilsson and

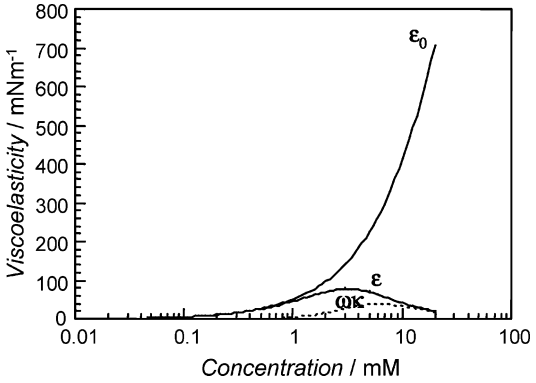

Figure 6. Complex elasticity (ϵ and $\omega\kappa$) and limiting elasticity (ϵ_o) for octyl β-glucoside surfactant. The diffusion coefficient used in the calculations was 3.73×10^{-10}.

Söderman, on the other hand, determined from NMR-self-diffusion experiments values of 3.64×10^{-10} and 3.97×10^{-10} m^2/s for the β-octyl-glucoside surfactant at 15 and 25 °C, respectively.[53,54]

On the basis of this information, and considering the translational self-diffusion coefficient equation for a sphere (eq 16),

$$D = \frac{k_B T}{6\pi\eta R_h} \tag{16}$$

Diffusion coefficients at 22 °C (for the monomeric beta surfactant) were estimated to be 3.73×10^{-10} m^2/s (eq 17).

$$D_{T_2} = D_{T1}\frac{\eta_{T_1} T_2}{\eta_{T_2} T_2} \tag{17}$$

here T refers to temperature and η the bulk viscosity of the aqueous solutions.

The diffusion coefficients at 22 °C for both the alpha and branched surfactants were estimated to be 4.98×10^{-10} m^2/s. Note that the diffusion coefficients for the alpha and branched surfactants were considered the same (no information is available for the branched surfactant) and their value was estimated from the ratio of diffusion coefficients for the beta and alpha surfactants by van Buuren and Berendsen.[52]

Figure 7 summarizes the results from the diffusional-relaxation model as applied to the C8β, C8α, and 2EHα surfactants (for a capillary wave of $k = 78\,507$ m^{-1}). At the studied frequencies some common features are observed for the elastic behavior, i.e., (1) there is a maximum in elasticity below the cmc, (2) agreement between the equilibrium elasticities and the calculated viscoelasticities takes place at concentrations below 1 mM, and, as expected, (3) the imaginary part of the complex dilatational modulus is smaller than the real part. No significant differences are seen for the viscoelasticity values predicted by the model for the studied species.

Evaluation of the Diffusion Model To Predict the Surface Rheological Behavior. The rheological parameters for soluble monolayers of the studied surfactants, as determined by SLS at 78508 m^{-1}, are included in Table 2.

As explained in the Experimental Section we also used polar plots in which the radial and semicircular lines represent constant (iso) interfacial elasticities and constant (iso) interfacial viscosities, respectively. The surface elasticity and viscosity can be estimated from the location of the experimental data within the polar plot. The procedure involved is unfortunately somewhat tedious because the rheological parameters are affected not only

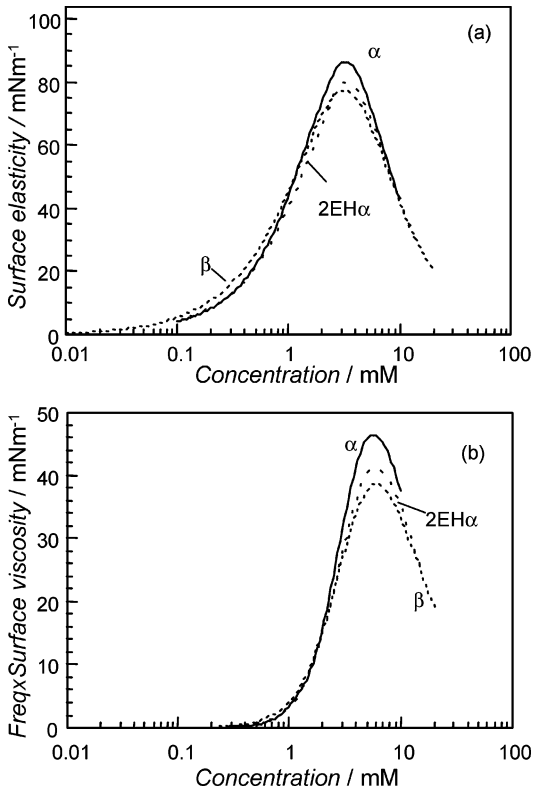

Figure 7. Real (a) and imaginary (b) part of the dilatational modulus for C8β (short space dotted line), C8α (continuous line), and 2EHα (long space dotted line) surfactants at 78 507 m^{-1}. The diffusion coefficients used in the calculations were 3.73×10^{-10}, 4.98×10^{-10}, and 4.98×10^{-10} m^2 s^{-1} for C8β, C8α, and 2EHα, respectively.

by the wavenumber but by the surface tension. An increase in surface tension also produces a shift to the right of the isoelast−isovisc pattern, which is more pronounced at higher surface pressures. Therefore, we present all the data obtained (from polar diagrams at each surface tension value) in a single, "overall" polar plot at a reference surface pressure ($\pi = 0$, in our case). This corresponding state approach was found to be a convenient way to interpret and compare rheological behavior in a wide variety of monolayer structures.[9,45]

Figure 8 shows the experimental loci of the viscoelastic behavior (in the form of polar diagrams) of the three surfactants at 78 508 m^{-1}. The corresponding plots for the other wavenumbers, i.e., 105 356 and 131 493 m^{-1}, show a similar

TABLE 2: Surface Elasticities (ϵ) and Surface Viscosities (κ) for the Studied Sugar Surfactants at 22 °C and k = 78 508 m^{-1}

concn, mM	ϵ, mN/m	κ, μg/s
octyl β-glucoside		
0.5	11	14
1	35	9
3	30	60
5	25	80
10	3.1	57
21	12	92
25	9.5	87
octyl α-glucoside		
0.5	19	45
1	34	45
3	42	-
10	12	95
2-ethylhexyl α-glucoside		
0.67	26.5	38
1.33	32.5	70
4.02	10	95
13.3	2.6	25

tendency (not reported for brevity). The polar plots show first the limiting case of a surfactant-free liquid dynamics (no monolayer present), i.e., pure water (π, C, ϵ, $\kappa = 0$). Between zero concentration and each of the lowest surfactant concentrations studied, there is uncertainty on the trajectory since no data are available, but definitely the tendencies indicate a deviation from the perfectly elastic film behavior ($\kappa = 0$ contour line). The maximum propagation velocity limit is attained in all cases at very dilute surfactant solutions. The maximum damping limit is also observed at low surfactant concentrations, before the minimum velocity limit at intermediate concentrations.

Interestingly, the polar plots shown in Figure 8 indicate small yet important differences in the viscoelasticity of the three isomeric (sugar) surfactants. Therefore, in agreement with other studies[55,56] it can be concluded that the stereochemistry of the surfactant plays an important role in molecular packing, intermolecular interactions, and the resulting macroscopic surface behaviors.

It is interesting to note that when comparing the results to those obtained for other non-ionic surfactants such as hexaethylenglycol mono-*n*-dodecyl ether ($C_{12}E_6$) (data not shown), a more "viscous" behavior is observed for the sugar-type surfactants (as judged from the trajectories of the experimental curves inside the polar diagram). Nevertheless, the values for surface

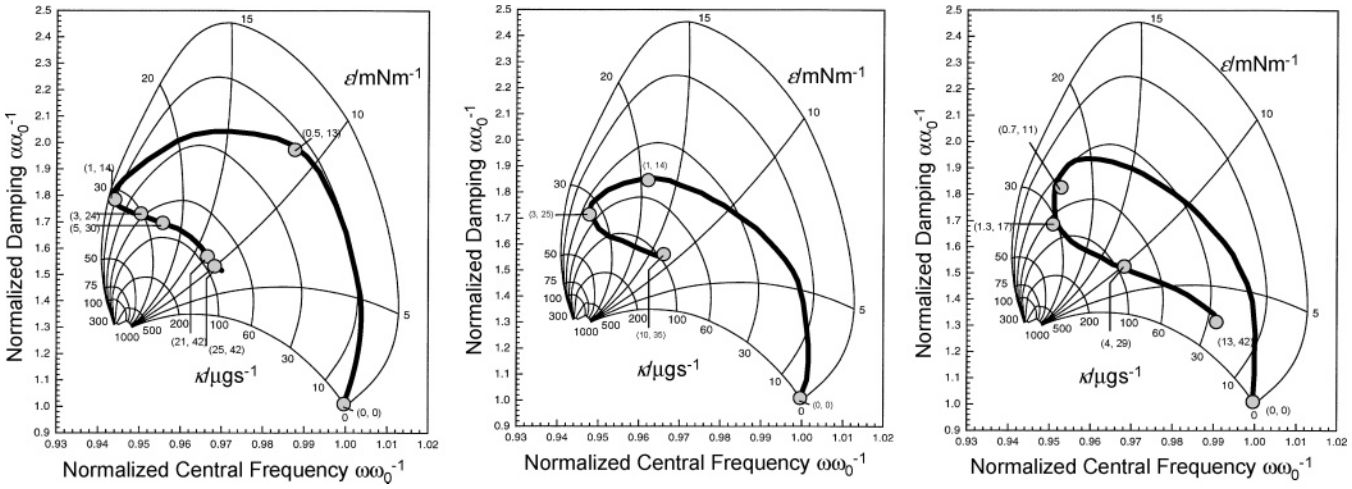

Figure 8. Polar plots and calculated loci of viscoelastic behavior for octyl β-glucoside (a), octyl α-glucoside (b), and 2-ethylhexyl α-glucoside (c) surfactants at $k_3 = 78\,508$ m^{-1} at a reference surface pressure $\pi = 0$ mN m^{-1}.

TABLE 3: Characteristic Relaxation Times (t_{rel}) and Experimental Times (t_{exp}) (for 3rd, 4th, and 5th Diffraction Orders) for Sugar Surfactants in the Peak Elasticity Region

surfactant	concn, mM	t_{rel}, μs	ω_0, kHz	t_{exp}, μs
C8β	2−6	2−50	20−500	7−7.5 (k_3)
C8α	3−5	3−23	44−333	4−5 (k_4)
2EHα	3−6	1−28	36−1000	3−3.5 (k_5)

viscosity are relatively small, indicating little lateral interactions between the adsorbed molecules.

A maximum in the surface elasticity and surface viscosity was observed for all the studied surfactants. A decrease in the surface elasticity with concentration has been reported in low-frequency studies[23,25,54] and has been interpreted in terms of the diffusional adsorption−dissolution model. It was previously argued that the adsorption−dissolution process is too slow to be "seen" by SLS experiments.[10] Using electrically excited capillary waves, Stenvot and Langevin[25] were able to demonstrate agreement between the diffusional model predictions and the measured elasticities. It seems that the failure to fit the diffusional model to data from SLS has driven efforts to study mechanically or electrically generated capillary waves rather than high-frequency thermal capillary waves. In the concentration range where the surface elasticity is highest the surface is almost saturated and therefore $d\Gamma/dC$ is smaller than that at the lower concentration region.

The values for the characteristic relaxation time t_{rel} can be calculated according to $t_{rel} = \omega_c^{-1}$ with ω_c from eq 6. These values are shown in Table 3 along with the characteristic experiment times, t_{exp}.

The relaxation time t_{rel} and experiment times t_{exp} are of similar magnitude and therefore it is concluded that it is possible to observe (or probe) the adsorption−dissolution process by using SLS. However, in the lower concentration region the relaxation time scale is in the order of milliseconds and therefore the surface behaves as a purely elastic surface, i.e., the relaxation process is too slow to be observed by these high-frequency experiments.

Figure 9a shows the experimental elasticities from SLS plotted together with values from the diffusional model. A good fit was observed only if a diffusion coefficient 10-fold higher than the expected value is used for the model calculations. More important than the differences between the diffusional coefficients is the fact that we observed a maximum in the elasticity that coincides with the range of values observed when using different diffusion coefficients in the model. Note that differences of up to 1000-fold for the experimental and the fitted diffusion coefficients have been observed by others.[25]

A similar discussion applies for the alpha surfactants (see Figure 9b). However, in this case the difference between the diffusion coefficients again is about 1 order of magnitude. Again, a maximum in surface elasticity is observed at around 1−3 mM surfactant concentration, well below the cm*c*. Figure 9c shows equivalent results for the branched surfactant, and in this case a larger discrepancy between the effective diffusion coefficient and bulk diffusion coefficient is observed. The noticeably larger diffusion coefficient for 2EHα is explained by the fact that the hydrophilic group of the surfactant is located near the center of the hydrophope. In other words, the shorter effective length of the tail in 2EHα produces a smaller effective radius (Rh) and therefore a larger diffusion coefficient.[57]

The fact that the "effective" diffusion coefficient is greater than the expected value can be attributed to the existence of thermal convection and other convective effects which may be included in the mass transfer balance of the diffusional−relaxation model. Also, relaxation processes within the monolayer, more specifically the existence of molecular rearrangements or other additional relaxation mechanisms, can be present. In any case, it is apparent that additional mechanisms take place next to the interface (throughout the characteristic thickness of the diffusion region) and therefore the diffusion coefficients usually calculated for bulk solution may not be appropriate. This latter hypothesis can be further elaborated after studying the characteristic length scale for the diffusion process. The monomer surfactants diffuse in the relaxation characteristic time to a distance of the order of $\Delta\Gamma/\Delta C$, which can be easily estimated from the respective surface excess plots to be of the order of 1−10 μm (for the medium-to-high concentration range).

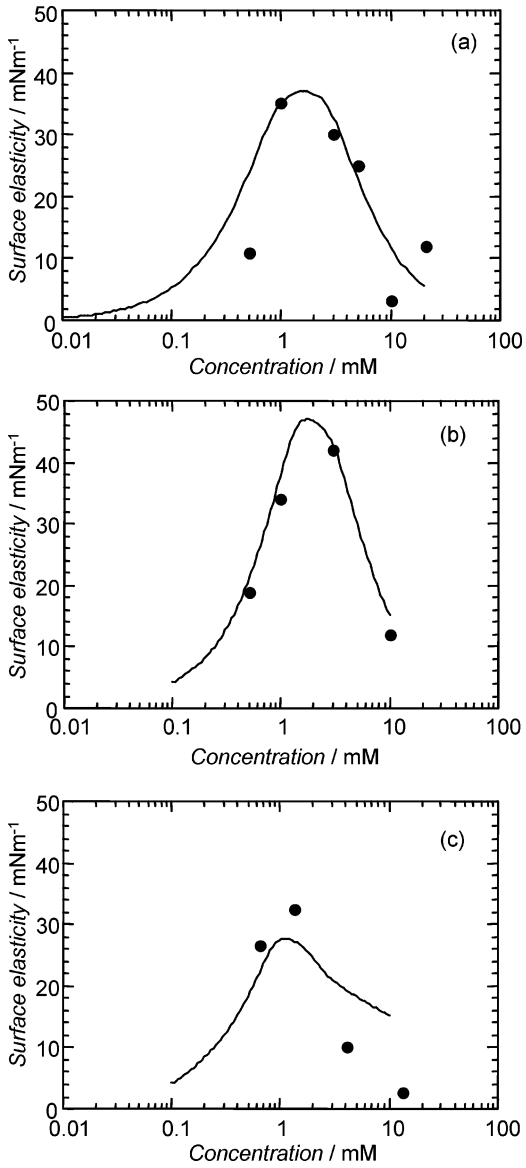

Figure 9. Experimental SLS (filled circles) and fitted elasticities (diffusional-relaxation model) for octyl β-glucoside (a), octyl α-glucoside (b), and 2-ethylhexyl α-glucoside (c) surfactant soluble monolayers. The diffusion coefficients used were 50×10^{-10}, 40×10^{-10}, and 200×10^{-10} m^2 s^{-1} for C8β, C8a, and 2EHα, respectively.

Conclusions

Accurate measurements of the characteristic parameters of capillary waves due to adsorption of surfactants at the air−water interface were successfully accomplished by surface light

scattering. Excellent agreement between the experimental results and predictions from hydrodynamic theory was achieved for pure water (with no excess damping).

The viscoelastic properties (surface elasticity and surface viscosity) of straight-chain (octyl β-glucoside and octyl α-glucoside) and branched-chain (2-ethylhexyl α-glucoside) non-ionic surfactant monolayers were quantified at submicellar concentrations. Differences in the viscoelastic behavior of these three isomers can be attributed to differences in stereochemistry, surface packing, and intermolecular interactions

It was shown that dynamic models for the exchange of surfactant between the surface and the bulk of the solution by diffusional relaxation describe qualitatively the trends observed in high-frequency, nonintrusive SLS. However, the quantitative departure of the experimental results from the theoretical predictions indicates the existence of additional effects not accounted for in the model that may involve molecular rearrangements and other relaxation mechanisms within the monolayer. Further research is underway to clarify these issues.

Acknowledgment. Financial support from the Strategic Research Foundation (SSF) program "Colloid and Interface Technology" is acknowledged. O.J.R. would also like to acknowledge The Faculty Internationalization Seed Grant Program at NCSU.

References and Notes

(1) Bos, M. A.; van Vliet, T. *Adv. Colloid Interface Sci.* **2001**, *91*, 437.
(2) Katyl, R. H.; Ingard, U. *Phys. Rev. Lett.* **1967**, *19*, 64.
(3) Earnshaw, J. C. *Adv. Colloid Interface Sci* **1996**, *68*, 1.
(4) Langevin, D. *Light Scattering by Liquid Surfaces and Complementary Techniques*; Marcel Dekker: New York, 1992; Vol. 41.
(5) Crawford, G. E.; Earnshaw, J. C. *Biophys. J.* **1987**, *52*, 87.
(6) Mandelstam, L. *Ann. Phys.* **1913**, *41*, 609.
(7) Braslau, A.; Pershan, P. S.; Swislow, G.; Ocko, B. M.; Alsnielsen, *J. Phys. Rev. A* **1988**, *38*, 2457.
(8) Skarlupka, R.; Seo, Y.; Yu, H. U. *Polymer* **1998**, *39*, 387.
(9) Hård, S.; Neuman, R. D. *J. Colloid Interface Sci.* **1987**, *120*, 15.
(10) Thominet, V.; Stenvot, C.; Langevin, D. *J. Colloid Interface Sci.* **1988**, *126*, 54.
(11) Kizling, J.; Stenius, P.; Eriksson, J. C.; Ljunggren, S. *J. Colloid Interface Sci.* **1995**, *171*, 162.
(12) Eastoe, J.; Sharpe, D. *Colloids Surf., A* **1998**, *143*, 261.
(13) Nickel, D.; Forster, T.; von Rybinski, W. In *Alkyl Polyglycoside, Technology, Properties and Applications*; Hill, K., von Rybinski, W., Stoll, G., Eds.; VCH: Weinheim, Germany, 1996.
(14) Watterson, J. G.; Elias, H. G.; Lasser, H. R. *Kolloid-Z. Z. Polym.* **1972**, *250*, 64.
(15) Tanaka, M.; Schiefer, S.; Gege, C.; Schmidt, R. R.; Fuller, G. G. *J. Phys. Chem. B* **2004**, *108*, 3211.
(16) Balzer, D. *Tenside, Surfactants, Deterg.* **1996**, *33*, 102.
(17) Lucassen-Reynders, E. H.; Lucassen, J. *Adv. Colloid Interface Sci.* **1969**, *2*, 347.
(18) Langevin, D. *Colloids Surf.* **1990**, *43*, 121.
(19) Miller, R.; Wustneck, R.; Kragel, J.; Kretzschmar, G. *Colloids Surf., A* **1996**, *111*, 75.
(20) Langevin, D. *Curr. Opin. Colloid Interface Sci.* **1998**, *3*, 600.
(21) Frumkin, A. N. *Z. Phys. Chem.* **1925**, *116*, 466.
(22) Lucassen, J.; Hansen, R. S. *J. Colloid Interface Sci.* **1967**, *23*, 319.
(23) Lucassen-Reynders, E. H. *Anionic Surfactants*; Marcel Dekker: New York, 1981; Vol. 11.
(24) Jayalakshmi, Y.; Ozanne, L.; Langevin, D. *J. Colloid Interface Sci.* **1995**, *170*, 358.
(25) Stenvot, C.; Langevin, D. *Langmuir* **1988**, *4*, 1179.
(26) Bonfillon, A.; Langevin, D. *Langmuir* **1993**, *9*, 2172.
(27) Szyszkowski, B. Z. *Phys. Chem.* **1908**, *4*, 385.
(28) Lucassen, J.; Hansen, R. S. *J. Colloid Interface Sci.* **1966**, *22*, 32.
(29) Lucassen, J.; Lucassen-Reynders, E. H. *J. Colloid Interface Sci.* **1967**, *25*, 496.
(30) van Voorst Vader, F.; Erkens, T. F.; van den Tempel, M. *Trans. Faraday Soc.* **1964**, *60*, 1170.
(31) Rayleigh, L. *Proc. R. Soc. London, Ser. A* **1890**, *48*, 127.
(32) Gibbs, J. W. *Collected Works*; Lonmans: Green, New York, 1928; Vol. 1.
(33) Levich, V. G. *Acta Physicochim. URSS* **1941**, *14*, 321.
(34) Levich, V. G. *Physicochemical Hydrodynamics*; Prentice Hall: Englewood Cliffs, NJ, 1962.
(35) Lamb, H. *Hydrodynamics*; Dover: New York, 1945.
(36) Djabbarah, N. F.; Wasan, D. T. *Chem. Eng. Sci.* **1982**, *37*, 175.
(37) Lucassen, J.; van den Tempel, M. *Chem. Eng. Sci.* **1972**, *27*, 1283.
(38) Hansen, R. S. *J. Appl. Phys.* **1964**, *35*, 1983.
(39) Hansen, R. S.; Mann, J. A. *J. Appl. Phys.* **1964**, *35*, 152.
(40) van den Tempel, M.; van de Riet, R. P. *J. Chem. Phys.* **1965**, *42*, 2769.
(41) Hård, S.; Neuman, R. D. *J. Colloid Interface Sci.* **1987**, *115*, 73.
(42) Bouchiat, M. A.; Meunier, J. *J. Phys.* **1971**, *32*, 561.
(43) Bellman, R.; Pennington, R. H. *Q. Appl. Math.* **1954**, *12*, 151.
(44) Kramer, L. *J. Chem. Phys.* **1971**, *55*, 2097.
(45) Esker, A. R.; Zhang, L. H.; Sauer, B. B.; Lee, W.; Yu, H. *Colloids Surf. A* **2000**, *171*, 131.
(46) Skarlupka, R. J.; Seo, Y.; Yu, H. *Macromolecules* **1997**, *30*, 953.
(47) Buzza, D. M. A.; Jones, J. L.; McLeish, T. C. B.; Richards, R. W. *J. Chem. Phys.* **1998**, *109*, 5008.
(48) Jiang, Q.; Chiew, Y.; Valentini, J. E. *J. Colloid Interface Sci.* **1993**, *155*, 8.
(49) Simister, E. A.; Thomas, R. K.; Penfold, J.; Aveyard, R.; Binks, B. P.; Cooper, P.; Fletcher, P. D. I.; Lu, J. R.; Sokolowski, A. *J. Phys. Chem.* **1992**, *96*, 1383.
(50) Matsumara, S.; Imai, K.; Yoshikawa, S.; Kawada, K.; Uchibori, T. *J. Am. Oil Chem. Soc.* **1990**, *67*, 996.
(51) Penfold, J.; Thomas, R. K. *J. Phys. Condens. Matter* **1990**, *2*, 1369.
(52) van Buuren, A. R.; Berendsen, H. J. C. *Langmuir* **1994**, *10*, 1703.
(53) Nilsson, F.; Söderman, O. *Langmuir* **1996**, *12*, 902.
(54) Nilsson, F.; Soderman, O.; Johansson, I. *J. Colloid Interface Sci.* **1998**, *203*, 131.
(55) Niraula, B. B.; Chun, T. K.; Othman, H.; Misran, M. *Colloids Surf. A* **2004**, *248*, 157.
(56) Neimert-Andersson, K.; Blomberg, E.; Somfai, P. *J. Org. Chem.* **2004**, *69*, 3746.
(57) Rosen, M. J. *Surfactants and Interfacial Phenomena*; Wiley: New York, 2004.